Evaluating the material parameters of the human cornea in a numerical model

WIESŁAW ŚRÓDKA*

Deformable Body Mechanics Faculty Unit, Wrocław University of Technology, Poland.

Purpose: The values of the biomechanical human eyeball model parameters reported in the literature are still being disputed. The primary motivation behind this work was to predict the material parameters of the cornea through numerical simulations and to assess the applicability of the ubiquitously accepted law of applanation tonometry – the Imbert–Fick equation.

Methods: Numerical simulations of a few states of eyeball loading were run to determine the stroma material parameters. In the computations, the elasticity moduli of the material were related to the stress sign, instead of the orientation in space.

Results: Stroma elasticity secant modulus E was predicted to be close to 0.3 MPa. The numerically simulated applanation tonometer readings for the cornea with the calibration dimensions were found to be lower by 11 mmHg then IOP = 48 mmHg.

Conclusions: This discrepancy is the result of a strictly mechanical phenomenon taking place in the tensioned and simultaneously flattened corneal shell and is not related to the tonometer measuring accuracy. The observed deviation has not been amenable to any GAT corrections, contradicting the Imbert–Fick law. This means a new approach to the calculation of corrections for GAT readings is needed.

Key words: *eyeball, biomechanical model, tonometry, IOP*

1. Introduction

The noninvasive intraocular pressure measurement techniques (developed for over a century) are based on strictly mechanical assumptions. Among them, the Goldmann applanation tonometry (GAT) features prominently [1], [2]. Also in the prognostication of refractive surgery optical effects, the eyeball is treated as a mechanical object [3], [4]. Hence natural are the attempts to solve such problems in the way peculiar to mechanical structures. The material parameters of eye shells are usually determined by carrying out in vitro laboratory tests on cadaver eyes [5]–[8]. Another technique is to numerically simulate in vitro or in vivo tests on the eyeball [9]–[13]. Instead of relying on direct laboratory measurements of stroma material parameters, a model is assigned an arbitrarily selected material to bring its mechanical functions close to the real ones. Simulation usually includes tonometry as well as the expansion of the eyeball or the cornea alone, affected by $p \equiv$ IOP (intraocular pressure). Attempts at comprehensive verification of experimental results by means of numerical models of the eyeball seem to be more successful considering that all the values of the secant elasticity modulus E obtained in this way are of the same order of magnitude. The calculated average values of E in a cornea subjected to nominal p amount to a few tenths of MPa [3], [11], [14], [15].

The aim of the present research was to predict the material parameters of the cornea through numerical simulation of three empirically well investigated states of eyeball loading (for which the results are readily available). The research has unexpectedly revealed that the mechanism of cornea apex flattening in GAT

is different than the one assumed so far and that the Imbert–Fick law on which applanation tonometry is based applies only to the nominal value of p.

1.1. Stroma mechanical parameter values reported in literature

Initially considered to be linear, the cornea material would be described using Young's modulus. The experimental values of this parameter fall within a very wide range: from 0.026 MPa [16] to 57 MPa [17]. The tensile graphs presented by UCHIO at al. [9] suggest even 115 MPa. The properties of exponential constitutive equation $\sigma = A[\exp(\alpha\varepsilon) - 1]$, where σ denotes the stress and ε stands for the strain, are discussed in the *Material* section. The coefficient A in the exponential equation usually does not exceed the range from 10^2 to 10^4 Pa while stiffening coefficient α assumes values from ten to around a hundred. From the measurements performed on samples cut from corneas NASH et al. [6] obtained exponent α values ranging from 34 to 82. For a cornea tested in vitro in the full eyeball WOO at al. [18] obtained $A = 5.4$ kPa and $\alpha = 28$. Later, Woo repeated the experiment, correcting the values to $A = 1.75$ kPa, $\alpha = 48.3$ (the data are quoted after: ETHIER et al. [19]). The review of the experimental results was done by FUNG [20].

1.2. Goldmann applanation tonometry

GAT is based on flattening the cornea apex over specified diameter D_{applan} and simultaneously measuring the needed force. The p_G pressure applied to the cornea from outside (a ratio of the force to the surface area) is the basis for determining the actual p in the eyeball [2]. The simplest expression of the relation between the two pressures is called the Imbert–Fick law:

$$p_G = p. \tag{1}$$

More detailed studies conducted later revealed departures from the Imbert–Fick law when central corneal thickness (CCT) differs from 0.520 mm [21] and when the corneal central radius of curvature differs from $R_{cornea} = 7.80$ mm [22]. Thus the Imbert–Fick law seems to be valid for only the so-called calibration dimensions of the eyeball:

$$\text{CCT} = 0.520 \text{ mm}, R_{cornea} = 7.8 \text{ mm},$$

$$D_{applan} = 3.06 \text{ mm}. \tag{2}$$

1.3. Ocular rigidity

When the volume of fluids in the eye increases by $\Delta V = V_2 - V_1$, intraocular pressure changes from p_1 to p_2. The pressure increase Δp to volume increase ΔV ratio is called eyeball rigidity. Function $p_2(\Delta V)$ is nonlinear and hence makes it difficult to compare the rigidities of different eyes. FRIEDENWALD [23] defined this eye parameter somewhat differently:

$$R_{eye} = \frac{\log(p_2) - \log(p_1)}{\Delta V}. \tag{3}$$

The above definition is still in use today and the attachment to it derives from the fact that the dependence of $\log(p_2)$ on ΔV is almost linear [24], [25]. This means R_{eye} independence of pressure whereby rigidity is described not by a function, but by a number and so it can be easily compared. More precise studies have shown that the R_{eye} parameter insignificantly depends on p, as well as on the initial eyeball volume V_1 [26], [27].

The rigidity R_{eye} measured by Friedenwald is within a range of 0.006–0.037 mm^{-3}, with an average of 0.0215 mm^{-3} [23]. The measurements were made on enucleated eyes. Later the tests were carried out on thousands of eyeballs by many other researchers, yielding similar results. The pressure was usually measured using the Goldmann tonometer. An extensive review of the studies was presented by NESTEROV at al. [27]. The use of calibration tables [28] reduced rigidity R_{eye} by over ten percent, i.e., to about 0.018 mm^{-3}. In vivo tests, using direct measurement of the pressure inside the eyeball, yielded even lower values of this parameter. Since the times of YTTEBORG [26] till today [29] the eye rigidity measured in this way has been close to 0.013 mm^{-3}. The lower value is explained by blood being squeezed out of the living eye's blood vessels as the pressure inside it increases. Therefore eye model volume change versus p should be compared with the results of in vitro measurements during which changes in eyeball volume are fully controlled.

2. Materials and methods

2.1. Eyeball model geometry

The model dimensions shown in table 1 conform to the ones recognized as standard in the literature

[30]. The difference is in the corneal geometry. Its profile (both anterior and posterior) is an ellipse

$$z(x) = \frac{1}{e^2 - 1} \cdot \left[\sqrt{R_0^2 + x^2 \cdot (e^2 - 1)} - R_0 \right] \qquad (4)$$

with eccentricity $e = 0.5$ [31].

The bases for selecting this function are the calculation results discussed by ASEJCZYK-WIDLICKA et al. [32].

Table 1. Eyeball model parameters

Parameter	Value
Axial radius of anterior corneal curvature	$R_0 = 7.8$ mm
Axial radius of interior corneal curvature	$r = 6.49$ mm
Central corneal thickness	CCT = 0.52 mm
Peripheral corneal thickness adjacent to limbus	PCT = 0.75 mm
Diameter of cornea	11.5 mm
Nominal intraocular pressure	$p = 16$ mmHg (2.14 kPa)

2.2. Material

In the eyeball biomechanical model, two material areas are distinguished: the cornea and the sclera. Each of the areas is assigned a homogenous, isotropic and nonlinear material. The isotropic material is a sufficiently accurate approximation of the tissue material, provided that the model simulates the intact cornea's field of strains [4].

As suggested by WOO et al. [5], [18], for calculations the following exponential function is most frequently assumed as the cornea material characteristic:

$$\sigma = A \left[\exp(\alpha \varepsilon) - 1 \right], \qquad \varepsilon \geq 0, \qquad (5)$$

where A and α are material constants. Tangential elasticity modulus $E_{\text{tangent}} = d\sigma/d\varepsilon$ is expressed by a linear stress function and at $\sigma \to 0$ it is different from zero:

$$E_0 = A\alpha. \qquad (6)$$

Exponential function (5) describes the material's behaviour under tension only, i.e., when $\varepsilon \geq 0$. For negative strain/stress the material is assumed to be subject to the linear physical law:

$$\sigma = E_0 \varepsilon, \qquad \varepsilon < 0. \qquad (7)$$

In the extreme version of such a material, referred to as a cable-type material, the stress for negative strain is equal to zero (Young's modulus $E_{\text{compress}} = 0$). The theoretical properties of membrane as described by the Laplace equation are derived from this type of material. When applied to the cornea's material, constitutive equation (7) reduces the cornea's flexural rigidity at a low p, making the model simulate the real cornea activity (i.e., makes the shell similar to the membrane).

Our studies of the eye model optical system [13] and WOO's et al. [18] experiments show that the ratio of the sclera to cornea secant elasticity moduli is

$$\frac{E_{\text{sec sclera}}}{E_{\text{sec cornea}}} \approx 5. \qquad (8)$$

This leads to the following constitutive equation for the sclera

$$\sigma = A(e^{5\alpha\varepsilon} - 1), \qquad \varepsilon \geq 0. \qquad (9)$$

For each of the models tested here, into which cornea material parameters A and α are introduced, the sclera material is described by equation (9) for $\varepsilon \geq 0$ and the stress is described by the law $\sigma = 5E_0\varepsilon$ for $\varepsilon < 0$ (in a way similar to that in (7)).

Poisson's ratio $\nu = 0.49$ is the same for all the materials in both zones.

2.3. Boundary conditions

There is no standard for eyeball model fixing. The two extreme cases of boundary conditions are: a simply supported model and a model fixed on the sclera's rear hemisphere. The actual boundary conditions are somewhere between the two. Our solutions for p_G differ slightly (by fractions of mmHg) between the two fixing modes [33] and so GAT simulations will be run for the simply supported model.

2.4. Numerical model

Displacement fields show axial symmetry during cornea applanation. For this reason, quadrilateral 8-node body-of-revolution elements (PLANE2D) were used to create a numerical model. The finite element modelling was implemented in the *Cosmos/M* system which is standard and commercially available software. The solution parameters take into account material curve asymmetry (the tension curve differs from the compression curve) and update the direction of pressure as structural deformations increase. The model is fully nonlinear, both physically and geometrically.

Intraocular pressure as a kinetic boundary condition was applied to the inner contour of the corneal–scleral shell using the standard Cosmos/M procedures. Corneal apex flattening in the GAT simulation was realized differently – as a kinematic condition, i.e., by shifting the nodes forming the outer outline of the corneal apex so that they would lie on a straight line perpendicular to the axis of symmetry. The external pressure was calculated after the solution, as the quotient of the resultant of the reactive force in the nodes at the applanation zone surface area. The flattening area each time was so extensive that none of the cornea profile nodes went through to the other side of the flattening surface and at the same time the forces in all the immobilized nodes were directed towards the cornea. By shifting in this way the applanation zone deeper into the eyeball, as it schematically indicated in figure 1, the next diameters and the corresponding external pressure values were obtained in the solutions. Pressure p_G was calculated (through interpolation) for a diameter of 3.06 mm.
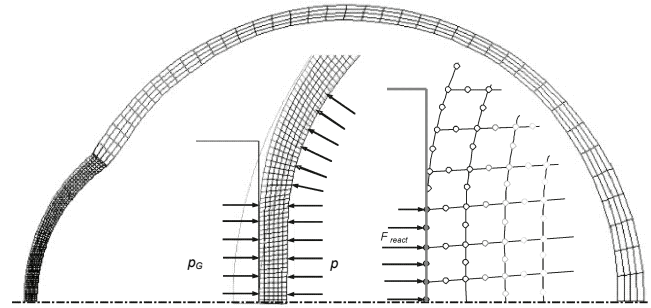

Fig. 1. Eyeball model finite element mesh and the view of corneal apex after flattening
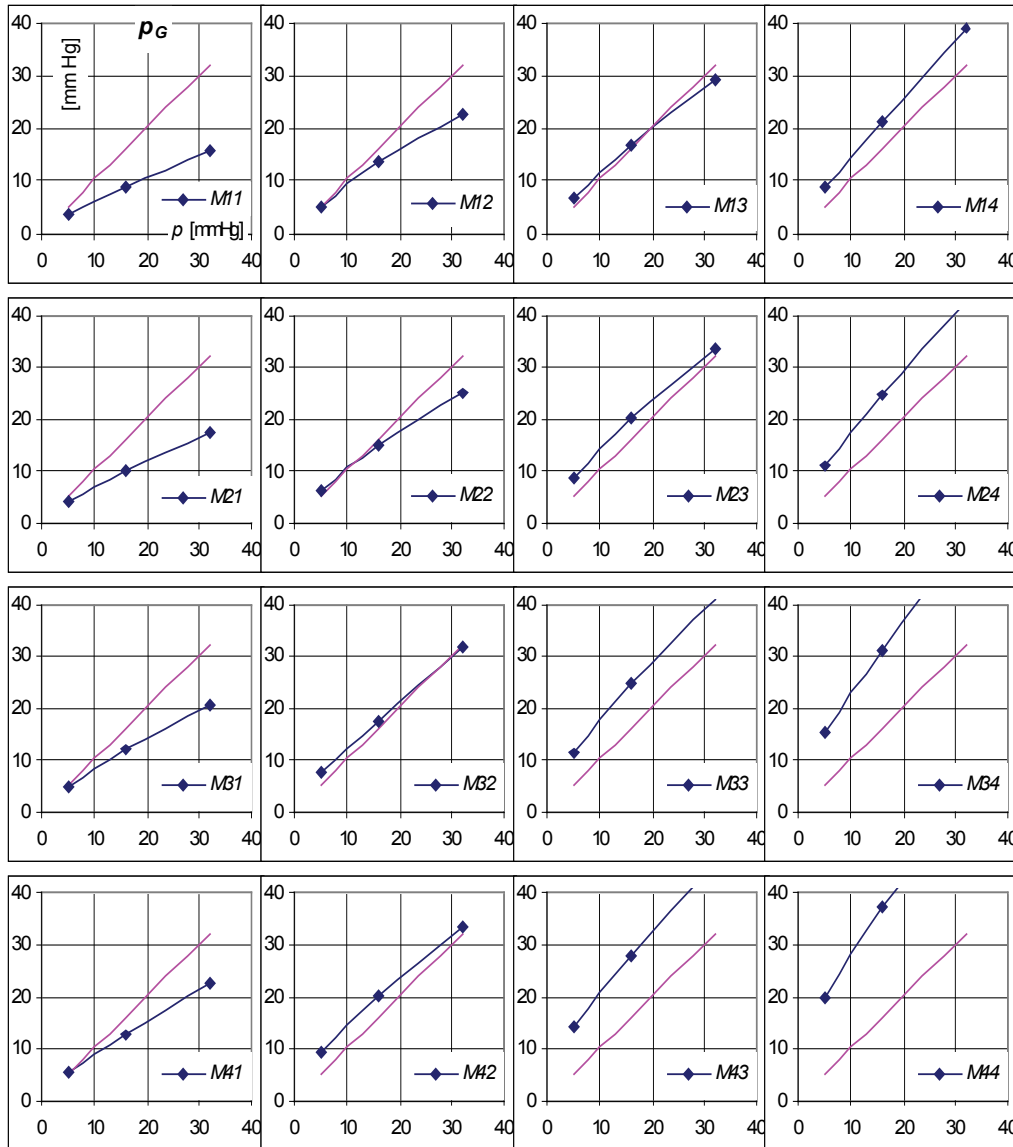

Fig. 2. Calculated applanation p_G as function of p for materials M_{ij} defined in tables 2 and 3

3. Results

3.1. GAT simulation

For testing purposes, a series of materials described by equations (5) and (7), and a linear material were selected. The object of the tests was the numerically calculated p_G pressure under the tonometer tip, depending on p and the material parameters. Initial material parameters A and α, ordered according to their values, are shown in table 2, while table 3 shows the symbols of the tested sixteen cornea materials M_{ij} created by combining A_i and α_j.

Table 2. Material parameters A and α
used to create M_{ij} characteristics

	A_i (MPa)	α_j
1	0.0001	30
2	0.0002	55
3	0.0005	90
4	0.0008	130

Table 3. Symbols of tested sixteen cornea materials M_{ij}
created by combining A_i and α_j

	α_1	α_2	α_3	α_4
A_1	M_{11}	M_{12}	M_{13}	M_{14}
A_2	M_{21}	M_{22}	M_{23}	M_{24}
A_3	M_{31}	M_{32}	M_{33}	M_{34}
A_4	M_{41}	M_{42}	M_{43}	M_{44}

The calculation results are presented in figure 2. They are arranged identically as the material designations in table 3 whereby changes in the p_G graphs caused by parameters A and α are clearly visible.

The relationship between material parameters A and α, leading to the satisfaction of the equation

$$p = p_G = 16 \text{ mmHg (2.14 Pa)}, \qquad (10)$$

is sought. A model with such a cornea material should behave in accordance with the Imbert–Fick law under the nominal pressure.

The results presented in figure 2 can be depicted as graphs of p_G (calculated for $p = 16$ mmHg) versus exponent α at fixed A. Four such graphs, for the successive values A_i given in table 2, are intersected with line $p_G = 16$ mmHg as shown in figure 3. In this way, four factors α (corresponding to each of the four parameters A) ensuring the satisfaction of equation (10) are determined.
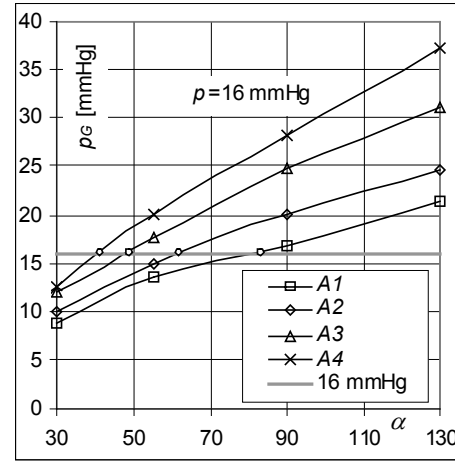

Fig. 3. "Measured" pressures of middle points ($p = 16$ mmHg)
of graphs shown in figure 2 for four successive values A_i,
depending on the exponent α. Intersection of functions
with straight line $p_G = 16$ mmHg allows one to determine values α
which ensure that $p_G = p = 16$ mmHg

The calculated material parameters are shown in table 4. The values are optimal for the GAT test. Besides factors A and α, table 4 contains initial modulus E_0 (at zero stress) and the value of secant module E_{secant} at a stress of 0.02 MPa. The stress close to the latter value (but biaxial) is present in the cornea apex at the nominal p.

Table 4. Optimal material parameters in GAT test

Material symbol	A (MPa)	α	E_0 (MPa)	E_{secant} (MPa)
M1	0.0001	83.0	0.0083	0.313
M2	0.0002	61.6	0.0123	0.267
M3	0.0005	47.7	0.0239	0.257
M4	0.0008	39.0	0.0312	0.239

The p_G pressure calculated for the models made of materials M1–M4, loaded with $p = 16$ mmHg, is very close to the actual pressure, as shown in figure 4. This proves that the four materials have been correctly matched. Completely new knowledge about the model emerges from the solutions for p other than nominal. Then (figure 4):

1. p_G proves to be a nonlinear function of p.

2. Below the nominal pressure (10), p_G is higher than p in each of the four cases.

3. Above the nominal pressure, p_G is lower than p regardless of the type of material.

4. At $p = 0$ the "measured" p_G pressure changes from 1.0 mmHg for M1 to 2.9 mmHg for M4. Above the zero value of p, the $p_G(p)$ curves do not differ noticeably in the investigated variation ranges of A and α.
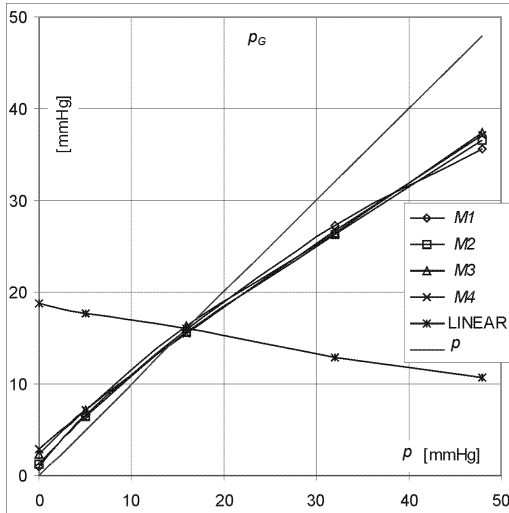
Fig. 4. Calculated applanation p_G versus p for models made
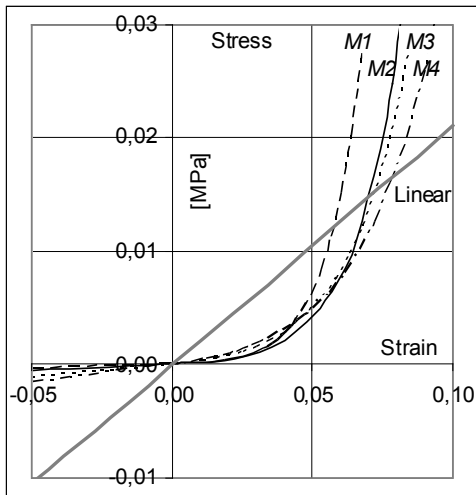of optimal materials M1–M4 and of linear material

the solution. Since there is no consensus among researchers as to the boundary conditions, calculations are done here for the two extreme cases: a simply supported eyeball and an eyeball fixed on its rear hemisphere. The actual support has to be somewhere in between.
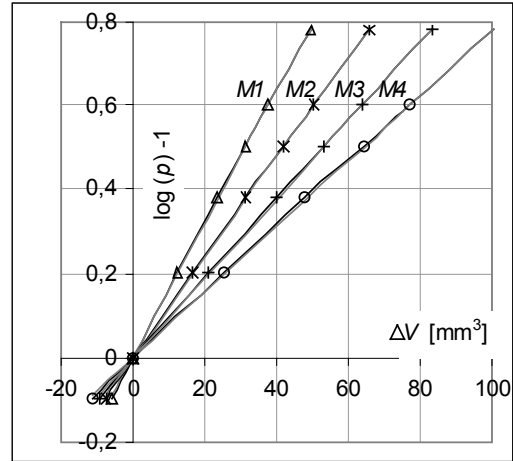

Fig. 6. Volumes calculated for simply supported model,
drawn in logarithmic scale.
Linear approximation of functions is also shown

Fig. 5. Curves for materials M1–M4 and for a linear material.
At compression, the stress–strain relationship
is governed by equation (5)

For comparison, also the linear model was solved. Young's moduli: $E_{\text{stroma}} = 0.21$ MPa and $E_{\text{sclera}} = 1.05$ MPa were assigned to its particular areas. At $E_{\text{stroma}} = 0.21$ MPa the model satisfies condition (10). Thus, despite the fact that the p_G function graph clearly differs from the other ones shown in figure 4, at a pressure of 16 mmHg the "measurement" result for the linear model is exactly the same as for all the other cases.

The characteristics of materials from M1 to M4, and of the linear one, are shown in figure 5.

3.2. Eyeball model rigidity

The model is tested by calculating its volume at increasing p. The method of support seriously affects

Volume change $\Delta V = V_2 - V_1$ is calculated relative to $V_1 = 6167$ mm^3 and $p_1 = 10$ mmHg. Thus, pressure on the logarithmic scale starts from 1. Since the Friedenwald definition of rigidity (3) does not take into account the shift of the graph along the axis of ordinates, let us shift the graphs one unit down so that they cross the origin of the coordinates as in figure 6.

Similar graphs, determined for the models fixed on the sclera's rear hemisphere, are shown in figure 7.
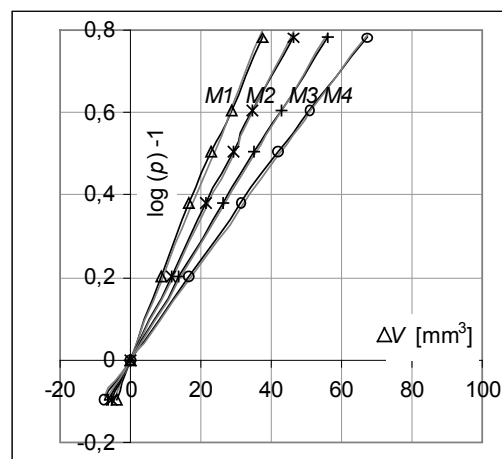

Fig. 7. Volumes calculated for model fixed
on sclera's rear hemisphere, drawn in logarithmic scale

The rigidities R_{eye} calculated for the two model support versions are presented in table 5.

Table 5. Rigidity coefficients calculated for eye models
simply supported or fixed on rear hemisphere

Material	R_{eye} (mm^{-3})		
	Simply supported	Fixed	Average
M1	0.0159	0.0211	**0.0185**
M2	0.0119	0.0171	**0.0145**
M3	0.0094	0.0140	0.0117
M4	0.0078	0.0118	0.0098

3.3. Test of cornea apex displacement under rising pressure

Calculations were performed for the fixed cornea model. The results are presented in figure 8. The graphs are shown against BRYANT and McDONNELL's [34] experimental curve.
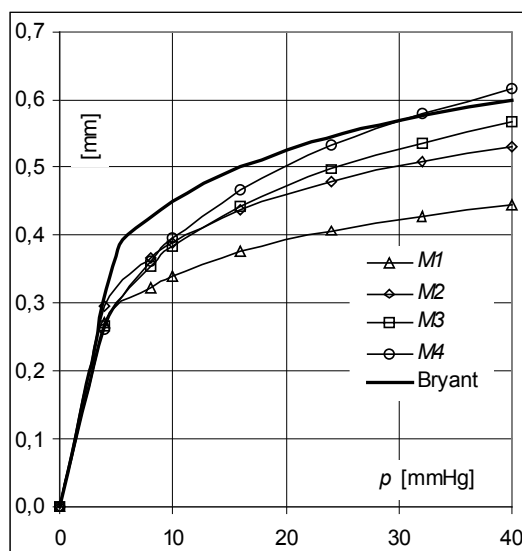

Fig. 8. Cornea apex displacements calculated for four models
made of materials M1–M4. Bryant & McDonnell's
experimental curve is shown for comparison

In numerical calculations, the location of the initial point of the corneal apex displacement does not pose a problem, as opposed to the interpretation of experimental results. The corneal area to be tested must be correctly defined and precisely excised. The zone around limbus attached to the preparation and the way of fixing it greatly affect the experimental result. One should take into account that the location of the origin of the experimentally determined graph is imprecisely defined, while the pressure applied to the cornea is known very precisely. This means that the Bryant and McDonnell's graph shown in figure 8 reflects the reality mainly in its shape and horizontal location, whereas its vertical location is less certain. Therefore

each of the graphs obtained from the models for the four verified materials is compared by shifting it vertically until it coincides with the experimental curve (figure 8). Undoubtedly, the best fit is for the line calculated for the M2 material model.

4. Discussion

4.1. Rigidity test

According to figures 6 and 7, R_{eye} depends on the boundary conditions. The calculations were performed for a simply supported eyeball and an eyeball fixed on its rear hemisphere. Experimental investigations of the fixing of the eye in the eye socket are scarce and ambiguous. KEMPF et al. [35] (2005) suggest an intermediate form of fixing. The extreme cases reported by them, however, indicate that one can find the sclera rigidly embedded in the surrounding tissues or simply supported. Since no eyeball support can be chosen on the basis of the experimental studies, the only solution is to calculate the arithmetic average of the results obtained for each of the assumed boundary conditions. A comparison of the numbers with experimental average $R_{eye} = 0.018$ (see the chapter on *Ocular rigidity*) favours the M1 and M2 materials.

4.2. Apex displacements

In the two tests: simulated GAT and simulated cornea apex displacement forced by pressure, the importance of the sclera and the limbus is small, while the cornea plays the principal role. The two tests determined the choice of material M2. The secant modulus of this material at a stress of 20 kPa amounts to $E = 0.267$ MPa and is close to the results obtained by other researchers [10], [14], [15], [18]. The significant difference lies in the fact that material M2 is much more nonlinear. Compression elasticity modulus E_0 in (6) amounts to merely 0.0123 MPa (table 4).

4.3. The p_G pressure is not a linear function of p pressure

The critical calculation results are shown in figure 4. The p_G functions for nonlinear materials have a characteristic shape relative to standard straight line (1). Undoubtedly, the result depends on equations (5) and

(7), and it leads to the extremely important conclusion: even the calibration eye model applied here does not satisfy the Imbert–Fick law within the tested physiological pressure range of 5–48 mmHg. If the model satisfies condition (10), then outside this point the "measured" p_G is clearly different from p – it is overestimated by about 2 mmHg at $p = 5$ mmHg and underestimated by about 11 mmHg at $p = 48$ mmHg. This discrepancy cannot be justified by the cornea model's flexural rigidity since the p_G required for flattening a cornea made of M1 and M2, at $p = 0$, amounts to merely 1 mmHg (figure 4). As the p load increases so does cornea tension, and p_G even smaller relative to p is sufficient to flatten the apex. At $p = 48$ mmHg, p_G amounts to merely 37 mmHg, and so it is lower than the pressure inside the eyeball and this obviously has no relation to shell flexural rigidity.

4.4. Relationship between the stress–strain material curve and the $p_G(p)$ function

The above results question the applicability of the Imbert–Fick law and warrant an investigation of the conditions to be satisfied by the cornea model material in order to obtain equal values of the calculated and actual p_G in the whole tested pressure range (i.e., up to 48 mmHg). The dependencies involved are presented as graphs in figure 9.
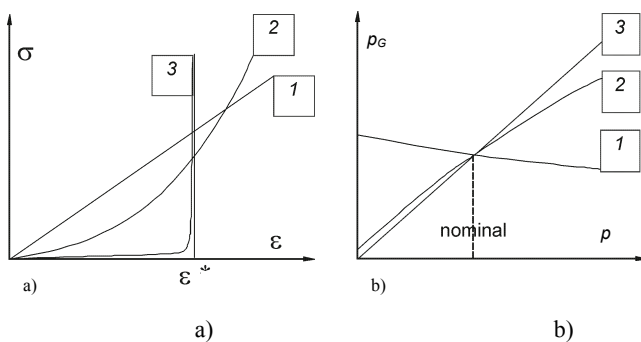

Fig. 9. Three types of cornea material curve (a).
$p_G(p)$ functions obtained for models made of materials with characteristics shown in figure 9a (b)

Curves marked with 1 and 2 in figure 9a,b correspond to the already described cases of the linear model and to the one made of the material with an exponential characteristic. Also a model which satisfies the Imbert–Fick law (1) in the p range tested here (line 3 in figure 9b) is possible, provided that a material with characteristics marked with 3 in figure 9a is used. The nonlinearity of this function is very high –

in the first stage (up to limit ε^*) the stress is close to zero, and at the limit itself it approaches infinity. Only then the eye model behaves in accordance with (1) (p_G directly proportional to p). Based on ORSSENGO and PYE's [14] thesis it can be concluded that elastic modulus E is proportional to the p load.

Tensile test curve 3 in figure 9a seems to be in disagreement with the results of experimental tests carried out on biological preparations, particularly on eye tissues [20]. Almost all literature data indicate characteristic 2 as proper for soft tissues (at least there is not much evidence pointing to characteristic 3).

It follows from the above analysis that either the calibration model made of the real material (5) is not strictly subject to law (1), or the law is satisfied but only by the model made of the unreal material with characteristic 3 shown in figure 9a. The author is in favour of the former alternative, but it also changes the hitherto conception of the mechanics of the phenomena accompanying GAT, as it indicates that p_G always differs from p, except for the nominal pressure, even when conditions (2) are satisfied. Some solutions to that phenomenon are given in [36].

4.5. Model ensuring merely $p_G = p = 16$ mmHg is usually faulty

In this context the p_G graph for the linear model from figure 4 is symptomatic. Loading the model with $p = 16$ mmHg and solving it one gets p_G equal to 16.0 mmHg. If the calculations were limited to one load value, one could regard the model as optimal. Its defectiveness becomes apparent only when one calculates p_G for other p loads. In the considered case, at $p = 0$, applanation p_G amounts to 18.7 mmHg. Thus the highest p_G is required for flattening the apex of a cornea made of a linear material when there is no p under the cornea. What happens then is equally surprising. As p is increased, p_G decreases instead of increasing. The model behaves completely differently from the real eye and unlike the nonlinear model. Loading the model with $p = 48$ mmHg leads to $p_G = 10.7$ mmHg – the lowest in the studied load range.

The result is symptomatic since it becomes apparent that solutions satisfying condition (10) can be obtained for arbitrary model geometry, boundary conditions and Young's modulus of the sclera by merely controlling Young's modulus of the cornea, as well as for arbitrary nonlinear materials having characteristics between 1 and 2 in figure 9a. This is an important observation since calculation results in numerous

publications are limited to only this single nominal pressure. The model can be forced to satisfy condition (10) regardless of the type of the material used, but only one particular material characteristic (curve 3 in figure 9a) ensures the satisfaction of condition (1) in the whole range of physiological pressure. However, this is not the stroma. A material having the characteristics needed for this purpose does not occur in the eye tissues.

References

[1] GOLDMANN H., SCHMIDT T., *Über Applanations-Tonometrie*, Ophthalmologica, 1957, 134, 221–242.

[2] GOLDMANN H., SCHMIDT T., *Weiterer Beitrag zur Applanationstonometrie*, Ophthalmologica, 1961, 141, 441–456.

[3] ALASTRUÉ V., CALVO B., PEÑA E., DOBLARÉ M., *Biomechanical modeling of refractive corneal surgery*, J. Biomech. Eng., 2006, 128(1), 150–160.

[4] YEH H.-L., HUANG T., SCHACHAR R.A., *A closed shell structured eyeball model with application to radial keratotomy*, J. Biomech. Eng., 2000, 122(5), 504–510.

[5] WOO S.L.-Y., KOBAYASHI A.S., LAWRENCE C., SCHLEGEL W.A., *Mathematical model of the corneo-scleral shell as applied to intraocular pressure–volume relations and applanation tonometry*, Ann. Biomed. Eng., 1972, 1(1), 87–98.

[6] NASH L.S., GREENE P.R., FOSTER C.S., *Comparison of mechanical properties of keratoconus and normal corneas*, Exp. Eye Res., 1982, 35, 413–423.

[7] DANIELSEN C.C., *Tensile mechanical and creep properties of Descemet's membrane and lens capsule*, Exp. Eye Res., 2004, 79, 343–350.

[8] ELSHEIKH A., ALHASSO D., RAMA P., *Assessment of the epithelium's contribution to corneal biomechanics*, Exp. Eye Res., 2008, 86, 445–561.

[9] UCHIO E., OHNO S., KUDOH J., AOKI K., KISIELEWICZ L.T., *Simulation model of an eyeball based on finite element analysis on a supercomputer*, Brit. J. Ophthalmol., 1999, 83, 1106–1111.

[10] ANDERSON K., EL-SHEIKH A., NEWSON T., *Application of structural analysis to the mechanical behavior of the cornea*, J. R. Soc. Lond. Interf., 2004, 1, 3–15.

[11] ELSHEIKH A., WANG D., KOTECHA A., BROWN M., GARWAY-HEATH G., *Evaluation of Goldmann applanation tonometry using a nonlinear finite element ocular model*, Ann. Biomed. Eng., 2006, 34(10), 1628–1640.

[12] PANDOLFI A., MANGANIELLO F., *A model for the human cornea: constitutive formulation and numerical analysis*, Biomechanics and Modeling in Mechanobiology, 2006, 5(4), 237–246.

[13] ŚRÓDKA W., PIERSCIONEK B.K., *Effect of material properties of the eyeball coat on optical image stability*, Journal of Biomedical Optics, 2008, 13(5), 054013.

[14] ORSSENGO G.J., PYE D.C., *Determination of the true intraocular pressure and modulus of elasticity of the human cornea*, B. Math. Biol., 1999, 61(3), 551–572.

[15] LIU J., ROBERTS C.J., *Influence of corneal biomechanical properties on intraocular pressure measurement*, J. Cataract. Refr. Surg., 2005, 31, 146–155.

[16] SJONTOFT E., EDMUND C., *In vivo determination of Young's modulus for the human cornea*, Bull. Math. Biol., 1987, 49, 217–232.

[17] ANDREASSEN T.T., SIMONSEN A.J., OXLUND H., *Biomechanical properties of keratoconus and normal corneas*, Exp. Eye Res., 1980, 31, 435–441.

[18] WOO S.L.-Y., KOBAYASHI A.S., SCHLEGEL W.A., LAWRENCE C., *Nonlinear material properties of intact cornea and sclera*, Exp. Eye Res., 1972, 14(1), 29–39.

[19] ETHIER C.R., JOHNSON M., RUBERTI J., *Ocular biomechanics and biotransport*, Ann. Rev. Biomed. Eng., 2004, 6, 249–273.

[20] FUNG Y.C., *Biomechanics: Mechanical Properties of Living Tissues*, Springer-Verlag, N.Y., 1993.

[21] EHLERS N.T., BRAMSEN T., SPERLING S., *Applanation tonometry and central corneal thickness*, Acta Ophthalmol., (Copenh.), 1975, 53, 34–43.

[22] BIER N., LOWTHER G.E., *Contact Lens Correction*, Butterworths, London, 1977.

[23] FRIEDENWALD J.S., *Contribution to the theory and practice of tonometry*, Am. J. Othalmol., 1937, 20, 985–1024.

[24] McEWEN W.K., St HELEN R., *Rheology of the human sclera: unifying formulation of ocular rigidity*, Ophthalmologica, 1965, 105, 321–346.

[25] SILVER D.M., GEYER O., *Pressure–volume relation for the living human eye*, Current Eye Research, 2000, 20, 115–120.

[26] YTTEBORG J., *The effect of intraocular pressure on rigidity coefficient in the human eye*, Acta Ophthalmol., 1960, 38, 548–561.

[27] NESTOROV A.P., BUNIN A.Y., KANTSELSON L.A., *Intraocular pressure* (in Russian), Nauka, 1974.

[28] NESTOROV A.P., VURGAFT M.B., *Calibration tables for the Filatov–Kalfa elastometer* (in Russian), Vestnik Ophth., 1972, 2, 20–25.

[29] PALLIKARIS I.G., KYMIONIS G.D., GINIS H.S., KOUNIS G.A., TSILIMBARIS M.K., *Ocular rigidity in living human eyes*, Invest. Ophthalmol. Vis. Sci., 2005, 46(2), 409–414.

[30] Le GRAND Y., El HAGE S.G., *Physiological Optics*, Springer Series in Optical Sciences, Vol. 13, New York, Springer-Verlag, Berlin, Heidelberg, 1980.

[31] KASPRZAK H., JANKOWSKA-KUCHTA E., *A new analytical approximation of corneal topography*, Journal of Modern Optics, 1996, 43, 1135–1148.

[32] ASEJCZYK-WIDLICKA M., ŚRÓDKA W., KASPRZAK H., ISKANDER D.R., *Influence of intraocular pressure on geometrical properties of a linear model of the eyeball: Effect of optical self-adjustment*, Optik, 2004, 115(11), 517–524.

[33] ŚRÓDKA W., *Effect of kinematic boundary conditions on optical and biomechanical behaviour of eyeball model*, Acta of Bioengineering and Biomechanics, 2006, 8(2), 69–77.

[34] BRYANT M.R., McDONNELL P.J., *Constitutive laws for biomechanical modeling of refractive surgery*, J. Biomech. Eng., 1996, 118, 473–481.

[35] KEMPF R., KURITA Y., IIDA Y., KANEKO M., MISHIMA H., TSUKAMOTO H., SUGIMOTO E., *Dynamic properties of human eyes*, Proceedings of the 2005 IEEE, Engineering in Medicine and Biology, 27th Annual Conference 2005, Shanghai, China, September 1–4.

[36] ŚRÓDKA W., *Goldmann applanation tonometry – not as good as gold*, Acta of Bioengineering and Biomechanics, 2010, 12(2), 39–47.